Report on a problem studied at the UK Mathematics-in-Medicine Study Group Loughborough 2008
< http://www.maths-in-medicine.org/uk/2008/orthopaedic-tissue/ >

8TH MATHEMATICS IN MEDICINE STUDY GROUP
LOUGHBOROUGH UNIVERSITY, 15–19 SEPTEMBER 2008

MODELLING OF THE GROWTH OF ENGINEERED ORTHOPAEDIC TISSUE IN ZERO FORCE AND VARIABLE LOAD ENVIRONMENTS

PROBLEM PRESENTED BY: HENK K. VERSTEEG

REPORT BY: CHRIS CATT DANIEL FRIEDRICH SHAILESH NAIRE

OTHER CONTRIBUTORS: JENNIFER BLOOMFIELD, CHRIS CATT, JOHN FOZARD, DANIEL FRIEDRICH, JOHN KING, YI-PING LO, SHAILESH NAIRE, COLIN PLEASE, JOHN WARD

(REPORT: [FEBRUARY 5, 2009] VERSION)

1 Introduction

The problem was presented to the study group by Henk Versteeg as part of the *remedi - Regenerative Medicine - A New Industry - Grand Challenge* project [1]. Regenerative medicine is a pioneering field that aims to create new treatments for diseases that result in the loss of major tissue function. An emerging therapy in regenerative medicine is tissue engineering. A striking definition of tissue engineering was by Langer and Vacanti [2], who stated it to be *an interdisciplinary field that applies the principles of engineering and life sciences toward the development of biological substitutes that restore, maintain, or improve tissue function or a whole organ.* The context of Henk's presentation was related to tissue engineering of the intervertebral disc (IVD).

The intervertebral discs lie between vertebrae in the human spine. They are connected to the vertebrae by cartilage filaments. The discs allow relative movement of the adjacent vertebrae and also act as shock absorbers. The IVD is the most avascular tissue in the human body, and its capacity to grow and repair itself is as low as articular cartilage [3]. Hence, nutrients for their regeneration have to be supplied from the adjacent vertebrae.

The IVD has two distinct anatomic regions (Figure 1). The annulus fibrosus (AF) forms the circumference of the IVD, and is composed of layers of fibrous cartilage which provide resistance to tensile and shear loads. The nucleus pulposus (NP) forms the central portion, and is jelly-like in form, providing resistance to compressive loading. Each region consists of chrondocytes (cells) surrounded by an abundant extracellular matrix (ECM) with different morphologies [3, 4]. The ECM comprises mainly of collagen, glycosaminoglycan (GAG) and water, and forms the main backbone of the tissue. GAG levels are generally considered as a good indicator of the overall quality of the ECM.

The functional ability of the IVD diminishes through age and general degeneration. Moreover, injury can lead to a hole in the AF which can cause significant loss of nucleus pulposus. The grand challenge is to use tissue engineering concepts to create a *viable* spinal disc construct which can then replace the damaged or diseased one. This is an area of intense research activity and several researchers have tried to engineer an IVD construct, for example, Sato *et al.* [5] have produced a high-density 3-D culture of AF cells to investigate IVD regeneration in white rabbits.

The tissue engineering process generally involves seeding the cells onto a biodegradable porous scaffold and providing adequate nutrients so that the cells can grow into a tissue. This set-up is cultivated in a bioreactor which provides a controlled environment for cell growth.

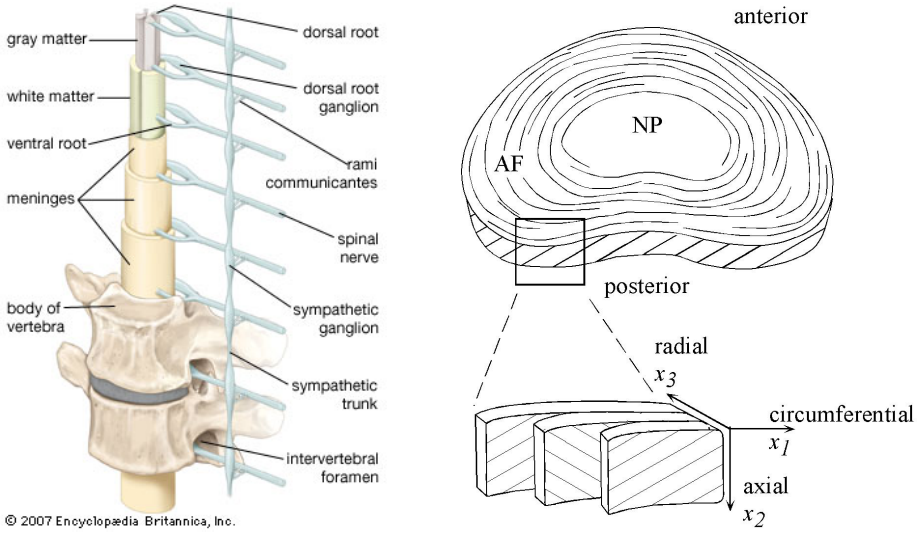

Figure 1: Left: schematic of the spinal cord from the Encyclopaedia Britannica. The intervertebral disc can be seen between the two vertebrae. Right: schematic of the intervertebral disc showing the annulus fibrosus and the nucleus pulposus.

Figure 2 is a schematic of the tissue engineering process in a rotating bioreactor. This poses a considerable challenge in both the experimental design (for example, in the manufacturing of a suitable scaffold) as well as in the optimization of the experimental parameters to grow a viable tissue. The latter is difficult due to different processes occurring at different timescales (for example, it takes around 10 days for the seeded cells to transform into GAG producing cells, while at least 6 weeks are required for the growth of sufficient tissue).

Mathematical and computational modelling can be a valuable tool in better understanding the various processes as well as in optimising the experimental parameters [6]. One such mathematical model was presented to the study group by Henk. The model was based on experimental data from Vunjak-Novakovic and Obradovic experiments [7] for creation of engineered

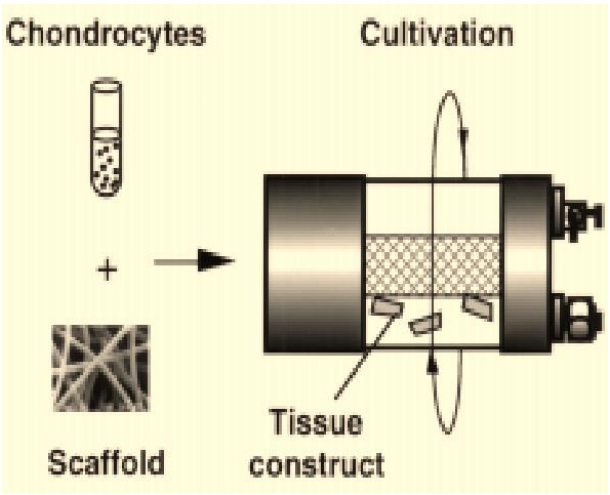

Figure 2: Cell-seeded scaffold cultured in a rotating bioreactor.

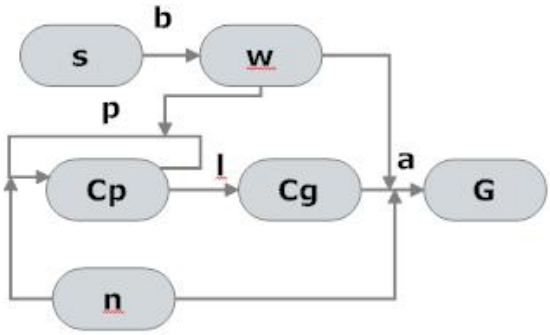

Figure 3: Diagram showing the connections between the model constituents, **s** = scaffold, **w** = water, **Cp** = proliferating cells, **Cg** = GAG producing cells, **G** = GAG and **n** = nutrients. The labels **p, a,b** and **l** represent rate constants, the latter 3 representing the model parameters α, β and λ, respectively.

cartilage by culture of bovine chrondcytes on biodegradable polymer scaffolds in bioreactors. These experiments provided data for the time evolution of cells and GAG which formed the basis of the model by Henk and co-workers.

This main aim of this study is

1. to incorporate the current understanding of processes controlling the cell seeding, cell proliferation, cell differentiation, GAG production and scaffold degradation into a *rational* mathematical model
2. to handle the moving boundary problem of the growing tissue construct
3. to optimise the experimental conditions of the bioreactor to grow a better quality tissue

2 Model Formulation

The model is based on mixture (or multiphase) theory [8], whereby each tissue component is treated on the macroscale as a continuum phase that occupies the same region of space. Mass and force balance equations are then written for each phase (with respect to their volume fractions), which determines their evolution. We do not consider the force balance in the model presented here. This will be investigated in future models. Mixture theory-type models have been used with reasonable success to understand the tissue engineering process [9, 10].

Figure 3 depicts the components of the system and their connections. The biodegradable scaffold (represented by its volume fraction s) is initially seeded with proliferating cells (represented by its volume fraction C_p). Nutrients (n represents the nutrient/oxygen concentration) dissolved in the culture medium (the culture medium is assumed to be mainly water, with volume fraction w) diffuse through the scaffold and is used by the cells to proliferate. The proliferating cells are observed to approximately double during the first 4 days after seeding [7]. These cells are then transformed into GAG producing cells (represented by its volume fraction C_g). This is observed to occur during the first 10 days of the experiment [7]. The production of GAG (represented by its volume fraction G) starts with the first GAG producing cells and increases up to day 10 when the full production rate is reached. The synthesised GAG pushes the cells and the scaffold apart leading to the gradual growth of the tissue construct. The tissue

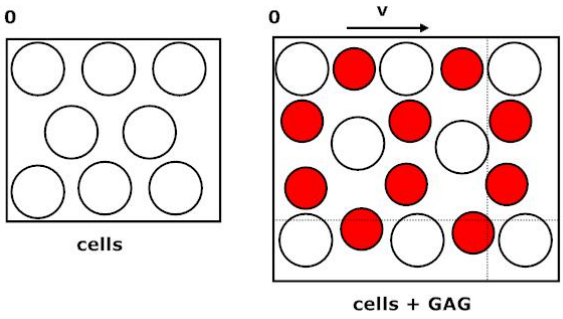

Figure 4: Diagram explaining the expansion of the tissue material. The cells (empty circles) produce GAG (red circles) which pushes the cells apart so that the tissue materials grows.

construct was observed to double in size over a period of 6 weeks [7]. This scenario is sketched in Figure 4. The scaffold, which initially occupies about 3% of the total volume, degrades to roughly 0.6% over the course of the experiment. For the purpose of our model, we will assume that the scaffold material degrades to water.

The scaffold geometry is a coin shaped polymer matrix with a diameter of 5 mm and a thickness of 1 mm [7]. The small aspect ratio makes it reasonable to consider only a 1D model, with the co-ordinate x along the thickness of the scaffold. Figure 5 shows a cross-section along the thickness of the scaffold. We assume symmetry about the origin. The moving boundary, representing the edge of the growing tissue construct, is represented by $L(t)$, where t is time.

We now translate the above processes into a mathematical model. The model is based on the convection, diffusion, production and depletion of each phase. Their equations can then be written as

$$\frac{\partial C_p}{\partial t} + \frac{\partial}{\partial x}\left(vC_p - D_{cp}\frac{\partial C_p}{\partial x}\right) = p\left[\frac{n}{n+B_0}\right]C_p - \lambda C_p(C_p+C_g), \tag{1}$$

$$\frac{\partial C_g}{\partial t} + \frac{\partial}{\partial x}\left(vC_g - D_{cg}\frac{\partial C_g}{\partial x}\right) = \lambda C_p(C_p+C_g), \tag{2}$$

$$\frac{\partial G}{\partial t} + \frac{\partial}{\partial x}\left(vG - D_G\frac{\partial G}{\partial x}\right) = \alpha C_g\left[\frac{n}{n+B_0}\right]\left[\frac{1}{G+G_c}\right], \tag{3}$$

$$\frac{\partial w}{\partial t} + \frac{\partial}{\partial x}\left(vw - D_w\frac{\partial w}{\partial x}\right) = -pC_p\left[\frac{n}{n+B_0}\right] - \alpha C_g\left[\frac{n}{n+B_0}\right]\left[\frac{1}{G+G_c}\right] + \beta s, \tag{4}$$

$$\frac{\partial s}{\partial t} + \frac{\partial}{\partial x}(vs) = -\beta s, \tag{5}$$

$$\frac{\partial n}{\partial t} + \frac{\partial}{\partial x}\left(vn - D_n\frac{\partial n}{\partial x}\right) = -\gamma(C_p+C_g)\left[\frac{n}{n+B_0}\right], \tag{6}$$

$$w + s + G + C_p + C_g = 1. \tag{7}$$

The first term on the LHS of equations (1 - 5) represent the rate of change of the volume fraction of each phase, the second term describes their convection and diffusion, while the terms on the RHS describe their production and depletion. The same description holds for equation (6) with the volume fraction replaced by the nutrient concentration. Equation (7) is a statement of volume conservation. The convective speed $v(x,t)$ of the mixture is related to the diffusivities of each phase. This can be realized by adding equations (1 - 5) and using equation (7).

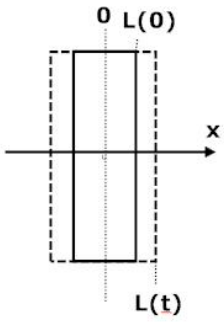

Figure 5: Geometry of the scaffold.

The expressions for the production and depletion of each species have been postulated based on the following ideas.

1. Cells proliferate by uptake of nutrients. Hence their production is dependent on the nutrients available (assumed proportional to the nutrient concentration).

2. This production rate is capped via a threshold nutrient concentration B_0, beyond which it levels out (represented by a Michaelis-Menten-type term).

3. Their depletion is due to transformation into GAG producing cells. This depends on the frequency of collisions between the cells (assumed to be proportional to the proliferating and GAG producing cells available). The same holds for the production of GAG producing cells.

4. The production of GAG is dependent on the availability of GAG producing cells and nutrients. This inverse dependence of the production on the GAG is to mimic the slowing down in production rate as more GAG is produced. Similar ideas hold for the production and depletion of water and scaffold.

5. We assume here that the scaffold biodegrades into water.

6. The depletion of nutrients depends on the proliferating and GAG producing cells consuming them (assumed to be proportional to each of the available cell-types).

The parameters in equations (1 - 7) are provided in Table 1.

3 The Non-dimensional Problem

We now non-dimensionalise the above equations. A characteristic time is based on a GAG production time scale, $\alpha^{-1} \approx 11$ days, a characteristic length scale is $L \approx 1$ mm, a characteristic speed is $\alpha L \approx 10^{-6}$ mm/s and a characteristic nutrient concentration (based on an initial concentration) is $n_0 \approx 10^{-10}$ mol/mm^3. Using these, we non-dimensionalise $t = \alpha^{-1}\tilde{t}$, $x = L_0\tilde{x}$, $v = \alpha L_0\tilde{v}$, $n = n_0\tilde{n}$. The non-dimensional equations are (dropping the $\sim$ on the variables)

Symbol	Parameter	Size	Units	Source
L	Thickness of the scaffold	1	mm	Henk
d	Diameter of the scaffold	5	mm	Henk
D_{cp}	Diffusion of proliferating cells	$10^{-7} - 10^{-6}$	$\mathrm{mm^2\,s^{-1}}$	Henk
D_{cg}	Diffusion of GAG producing cells	10^{-11}	$\mathrm{mm^2\,s^{-1}}$	[7]
D_n	Diffusion of oxygen	3×10^{-3}	$\mathrm{mm^2\,s^{-1}}$	Henk
D_G	Diffusion of GAG	7×10^{-9}	$\mathrm{mm^2\,s^{-1}}$	[7]
D_w	Diffusion of water	$10^{-5} - 10^{-3}$	$\mathrm{mm^2\,s^{-1}}$	guess
α	GAG production rate	10^{-6}	$\mathrm{s^{-1}}$	[7]
λ	GAG cell production rate	10^{-6}	$\mathrm{s^{-1}}$	[7]
β	scaffold degradation rate	10^{-6}	$\mathrm{s^{-1}}$	[7]
p	cell proliferation rate	2.5×10^{-6}	$\mathrm{s^{-1}}$	[7]
γ	oxygen consumption rate	10^{-12}	$\mathrm{mol\,mm^{-3}\,s^{-1}}$	[7]
B_0	threshold oxygen concentration	6×10^{-6}	$\mathrm{mol\,l^{-1}}$	Henk
n_0	initial oxygen concentration	10^{-10}	$\mathrm{mol\,mm^{-3}}$	Henk
C_{p0}	initial cell volume fraction	0.5	1	guess
s_0	initial scaffold volume fraction	0.03	1	[7]

Table 1: Parameters and their estimates

$$\frac{\partial C_p}{\partial t} + \frac{\partial}{\partial x}\left(vC_p - \tilde{D}_{cp}\frac{\partial C_p}{\partial x}\right) = \tilde{p}\left[\frac{n}{n+\tilde{B}_0}\right]C_p - \tilde{\lambda}C_p(C_p+C_g), \tag{8}$$

$$\frac{\partial C_g}{\partial t} + \frac{\partial}{\partial x}\left(vC_g - \tilde{D}_{cg}\frac{\partial C_g}{\partial x}\right) = \tilde{\lambda}C_p(C_p+C_g), \tag{9}$$

$$\frac{\partial G}{\partial t} + \frac{\partial}{\partial x}\left(vG - \tilde{D}_G\frac{\partial G}{\partial x}\right) = C_g\left[\frac{n}{n+\tilde{B}_0}\right]\left[\frac{1}{G+G_c}\right], \tag{10}$$

$$\frac{\partial w}{\partial t} + \frac{\partial}{\partial x}\left(vw - \tilde{D}_w\frac{\partial w}{\partial x}\right) = -\tilde{p}C_p\left[\frac{n}{n+\tilde{B}_0}\right] - C_g\left[\frac{n}{n+\tilde{B}_0}\right]\left[\frac{1}{G+G_c}\right] + \tilde{\beta}s, \tag{11}$$

$$\frac{\partial s}{\partial t} + \frac{\partial}{\partial x}(vs) = -\tilde{\beta}s, \tag{12}$$

$$\frac{\partial n}{\partial t} + \frac{\partial}{\partial x}\left(vn - \tilde{D}_n\frac{\partial n}{\partial x}\right) = -\tilde{\gamma}(C_p+C_g)\left[\frac{n}{n+\tilde{B}_0}\right], \tag{13}$$

$$w + s + G + C_p + C_g = 1. \tag{14}$$

The dimensionless parameters and their estimates are provided in Table 2. Some of the estimates were obtained from Obradovic *et al.* [7] and Henk Versteeg's presentation to the study group.

Based on the parameter estimates, further simplification of the above equations is possible. Unfortunately, there is a lot of uncertainty in the accuracy of some of the parameters obtained from literature. For example, the GAG molecules are large and hence intutively GAG diffusion is likely to be very slow. However, accurate data of GAG diffusivity was not found and so the GAG diffusion is retained in the equations. One simplification that is possible relates to the diffusivity and the consumption rate of nutrient/oxygen molecules. These molecules are very small and thus diffuse rapidly. Moreover, they are also consumed rapidly relative to the quantity of GAG produced. Hence, diffusion of oxygen and its consumption dominate the other terms in equation (13). The scaffold does not degrade substantially in the time scale of interest

Symbol	Definition	Size
$\tilde{p}$	p/α	2.5
$\tilde{\lambda}$	λ/α	1
$\tilde{\beta}$	β/α	1
$\tilde{\gamma}$	$\gamma/(\alpha n_0)$	10^4
$\tilde{B}_0$	B_0/n_0	6×10^{-2}
$\tilde{D}_{cp}$	$D_{cp}/(\alpha L^2)$	$0.1 - 1$
$\tilde{D}_{cg}$	$D_{cg}/(\alpha L^2)$	0
$\tilde{D}_n$	$D_n/(\alpha L^2)$	1.5×10^3
$\tilde{D}_G$	$D_G/(\alpha L^2)$	7×10^{-3}
$\tilde{D}_w$	$D_w/(\alpha L^2)$	$10^2 - 10^3$

Table 2: Non-dimensional parameters of the system

(it degrades to about a fifth of its initial volume in about 6 weeks). Therefore, we neglect the influence of the scaffold in this problem. The reduced system can be written as follows

$$\frac{\partial C_p}{\partial t} + \frac{\partial}{\partial x}\left(vC_p - \tilde{D}_{cp}\frac{\partial C_p}{\partial x}\right) = \tilde{p}\left[\frac{n}{n+\tilde{B}_0}\right]C_p - \tilde{\lambda}C_p(C_p + C_g), \tag{15}$$

$$\frac{\partial C_g}{\partial t} + \frac{\partial}{\partial x}\left(vC_g - \tilde{D}_{cg}\frac{\partial C_g}{\partial x}\right) = \tilde{\lambda}C_p(C_p + C_g), \tag{16}$$

$$\frac{\partial G}{\partial t} + \frac{\partial}{\partial x}\left(vG - \tilde{D}_G\frac{\partial G}{\partial x}\right) = C_g\left[\frac{n}{n+\tilde{B}_0}\right]\left[\frac{1}{G+G_c}\right], \tag{17}$$

$$\tilde{D}_n\frac{\partial^2 n}{\partial x^2} = -\tilde{\gamma}(C_p + C_g)\left[\frac{n}{n+\tilde{B}_0}\right], \tag{18}$$

$$\frac{\partial v}{\partial x} = \tilde{D}_{cp}\frac{\partial^2 C_p}{\partial x^2} + \tilde{D}_{cg}\frac{\partial^2 C_g}{\partial x^2} + \tilde{D}_G\frac{\partial^2 G}{\partial x^2} + \tilde{D}_w\frac{\partial^2 w}{\partial x^2}, \tag{19}$$

$$w = 1 - C_p - C_g - G. \tag{20}$$

Note that we have replaced the equation for the volume fraction of water with that for the convective speed of the mixture.

4 Boundary and Initial Conditions

The boundary conditions imposed on the above equations are as follows. We assume symmetry at $x = 0$. Hence,

$$\frac{\partial C_p}{\partial x} = \frac{\partial C_g}{\partial x} = \frac{\partial n}{\partial x} = \frac{\partial G}{\partial x} = v = 0, \quad \text{at} \quad x = 0. \tag{21}$$

We consider two sets of boundary conditions at $x = L(t)$.

$$\mathcal{Q}_{C_p} = C_p\frac{dL}{dt}, \qquad \mathcal{Q}_{C_g} = C_g\frac{dL}{dt}, \qquad \mathcal{Q}_G = QG + G\frac{dL}{dt}, \qquad n = 1, \tag{22}$$

and

$$C_p = C_g = G = 0, \qquad w = 1, \qquad n = 1, \tag{23}$$

where

$$\mathcal{Q}_{C_p} = vC_p - \tilde{D}_{cp}\frac{\partial C_p}{\partial x}, \qquad \mathcal{Q}_{C_g} = vC_g - \tilde{D}_{cg}\frac{\partial C_g}{\partial x}, \qquad \mathcal{Q}_G = vG - \tilde{D}_G\frac{\partial G}{\partial x} \tag{24}$$

are the flux of proliferating and GAG producing cells, and GAG, respectively. The first two conditions in equation (22) imply that there is no flux of proliferating and GAG producing cells out of the tissue construct, relative to the moving boundary. However, we allow a flux of GAG (assumed proportional to the GAG volume fraction with proportionality constant $Q > 0$) to leave the tissue construct, relative to the moving boundary. This mimics the "washing away" of GAG. Due to volume conservation, this loss of GAG is replaced by water from the surrounding culture medium. The second set of boundary conditions, in equation (23) are chosen based on the fact that at the tissue construct edges there is an infinite reservoir of water available via the culture medium. The boundary condition on the nutrient concentration, used in both sets of boundary conditions, assumes an infinite supply of nutrients from the culture medium outside the tissue construct. The kinematic condition, $v(x = L(t)) = \dfrac{dL}{dt}$, is used to evolve the tissue construct boundary. Using this and the above defined fluxes, the first three boundary conditions in equation (22) can be then simplified to

$$\frac{\partial C_p}{\partial x} = \frac{\partial C_g}{\partial x} = 0, \quad -\tilde{D}_G\frac{\partial G}{\partial x} = QG. \tag{25}$$

The initial conditions chosen are;

at t=0;

$$C_p = C_{p_0}, \quad C_g = 0, \quad G = 0 \quad s = s_0, \quad w = 1 - C_{p_0} - s_0, \quad L = 1. \tag{26}$$

This mimics the scenario in which an initially uniform distribution of scaffold seeded cells are allowed to evolve.

5 Results

For the purposes of the numerical solution, we find it convenient to transform the domain $0 \leq x \leq L(t)$ to a fixed domain $0 \leq \xi \leq 1$, using the transformation $\xi = \dfrac{x}{L(t)}$. Using this change of variable, we find that;

$$\frac{\partial}{\partial t} = \frac{\partial}{\partial t} - \frac{\xi}{L}\frac{dL}{dt}\frac{\partial}{\partial \xi}, \tag{27}$$

$$\frac{\partial}{\partial x} = \frac{1}{L}\frac{\partial}{\partial \xi}, \tag{28}$$

and

$$\frac{\partial^2}{\partial x^2} = \frac{1}{L^2}\frac{\partial^2}{\partial \xi^2}. \tag{29}$$

The modified system of equations are then solved numerically ensuring that they are in conservation form. A centered finite difference scheme is used for the spatial derivatives. A

Parameter	Value
$\tilde{p}$	0.1
$\tilde{\lambda}$	2
$\tilde{\gamma}$	1
$\tilde{D}_{cp}$	0.01
$\tilde{D}_{cg}$	0.01
$\tilde{D}_n$	1
$\tilde{D}_G$	0.01
$\tilde{D}_w$	1

Table 3: Non-dimensional parameters used in numerics

backward Euler discretization is used to advance the system in time. For the initial attempt at solving the system of equations some of the parameters in table 2 were modified. These are shown in table 3.

We first present the results using the boundary conditions in equation (22). Figures 6 (a),(b) and (c) show the distribution of proliferating and GAG producing cells, and GAG after 0, 20 and 42 days, respectively. The proliferating cells are observed to uniformly decrease in time (approximately 90% depletion in 42 days), as they are converted into GAG producing cells. This subsequently increases the GAG producing cells, which in turn increases the GAG production. Figure 6 (d) shows the nutrient distribution after 42 days. There is a sufficient supply of nutrients near the tissue construct edge. However, in the center of the tissue construct, there is severe depletion of nutrients (depletes to approximately a tenth of its initial value). This is due to their intake by GAG producing cells to produce GAG, which is maximum near the tissue construct center (see Figure 6 (b),(c)). This would need to be monitored in order to prevent the center of the tissue construct from being completely starved of nutrients, before appreciable levels of GAG have been produced. Figure 6 (e) shows the evolution of the tissue construct thickness L in time. After an initial phase of insignificant growth (about 5 days), the tissue construct thickness is observed to increase almost linearly in time. It grows to almost three times its initial thickness in about 42 days. This is more than that observed in experiments (doubles in size in 42 days [7]), which suggests that the value of the GAG production rate parameter α is greater than it should be. The rate of growth of the tissue construct v as a function of position is shown in Figure 6 (f). It is also observed to vary almost linearly with position, with the maximum growth rate near the tissue construct edge.

The results using the boundary conditions in equation (23) are presented in Figure 7. The same trends are observed here as in the earlier case. The only marked difference is in the initial growth of the tissue construct, which is quite dramatic for this case (see Figure 7 (e)). The tissue construct is seen to double in size in about 10 days, in contrast to the earlier case where insignificant growth is observed in the same amount of time. As described in Section 4, the construct, for this case, is entirely surrounded by water. At least during the initial stage, the water diffuses rapidly into the construct resulting in significant growth.

6 Conclusions and Future Work

We were presented with a model by Henk and co-workers for growing engineered orthopaedic tissue based on experimental data [7]. We pin-pointed several ambiguities in their model, in particular, with the expressions used in their GAG production. Our main goal was to derive a rational model which would facilitate better understanding of the physical processes involved

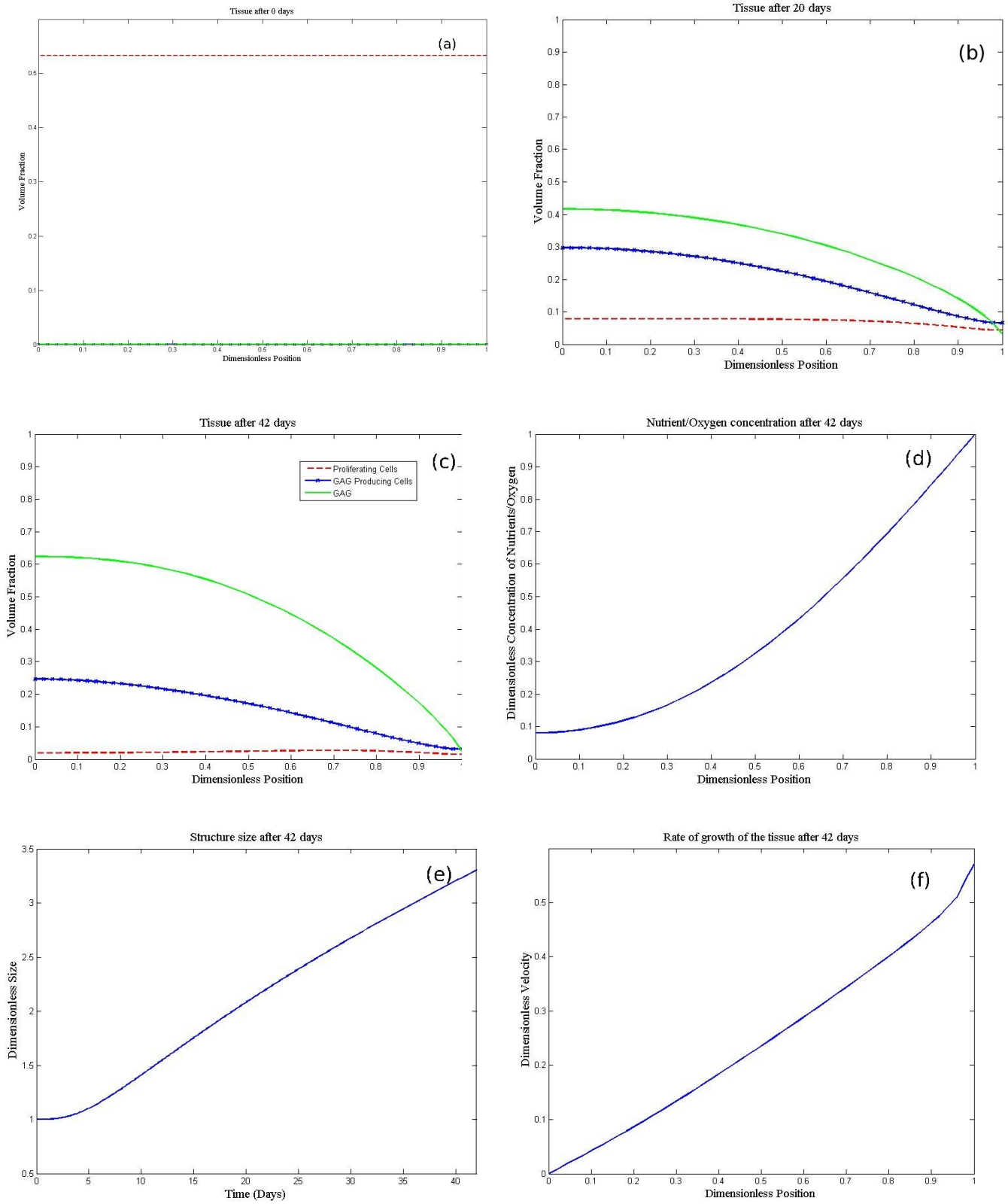

Figure 6: Results using the boundary conditions in equation (22). Graphs show cell and GAG volume fractions after (a) 0, (b) 20 and (c) 42 days, (d) nutrient concentration after 42 days, (e) tissue construct size versus time and (f) the rate of tissue growth after 42 days.

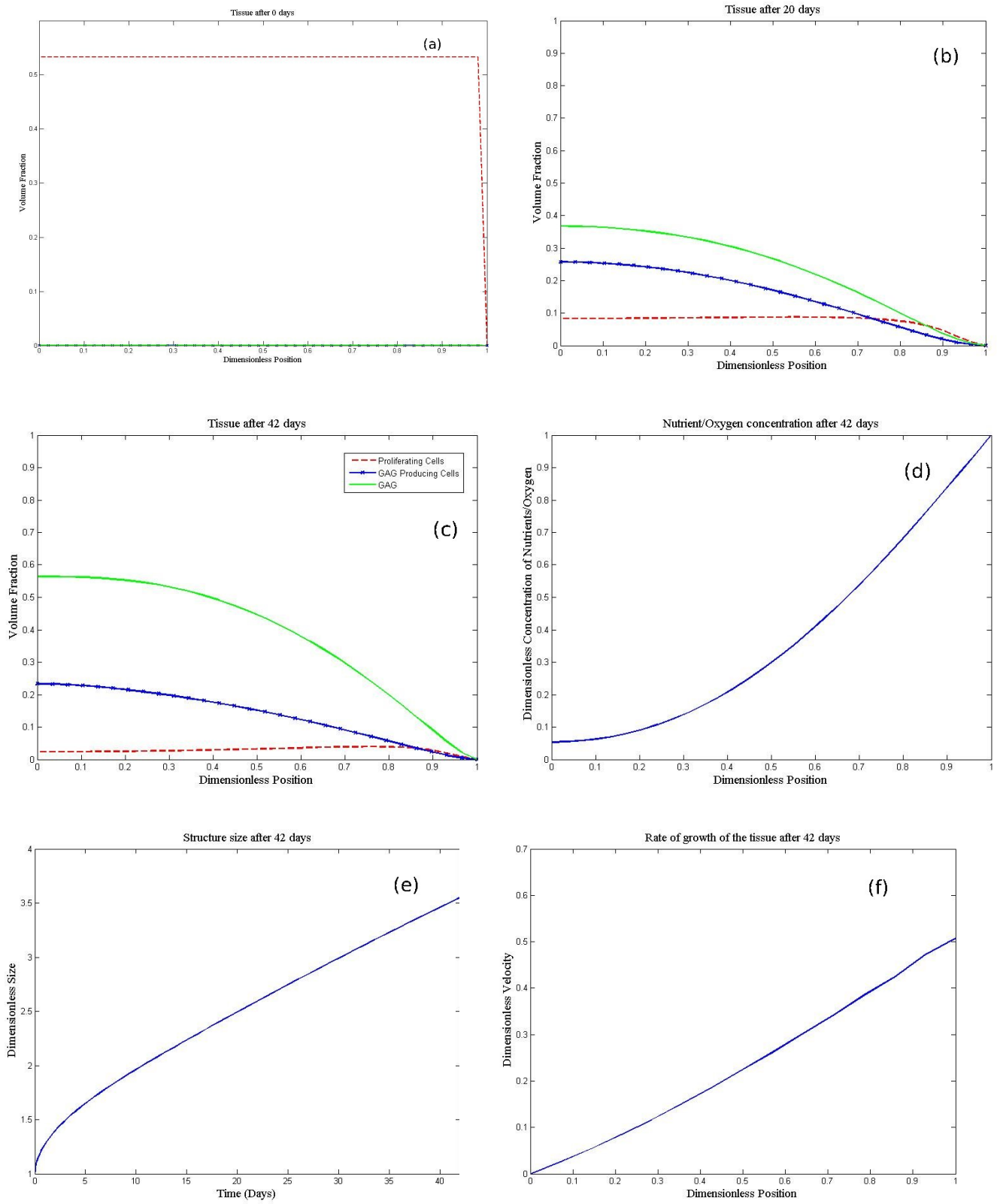

Figure 7: Results using the boundary conditions in equation (23). Graphs show cell and GAG volume fractions after (a) 0, (b) 20 and (c) 42 days, (d) nutrient concentration after 42 days, (e) tissue construct size versus time and (f) the rate of tissue growth after 42 days.

as well as in reflecting the in vitro results [7]. The model accounts for GAG production due to cell uptake of nutrients as well as due to the changing cell characteristics (from proliferation to GAG producing) at different time periods. The novelty in our model was in the treatment of cells as two distinct entities, i.e., proliferating and GAG producing. This facilitated the transfer of proliferating cells into GAG producing cells which is important in controlling GAG production subsequently influencing the growth of the tissue construct. The role of water via the culture medium, in how it flows through the construct and its use in cell proliferation and GAG production, was also catered for. Scaffold degradation was initially included in the model but was omitted due to its negligible effect on the essential dynamics of the growing construct.

The model successively captures several qualitative features of the tissue engineering process observed in experiments [7]. However, for better quantitative comparison, an adjustment in the parameters is required. For example, experimental observations showed that cells proliferate only in the first four days and the production of GAG is initiated after 12 days. Our model accommodates for this through a specified transfer rate (represented by the parameter λ) between proliferating and GAG producing cells. The value of λ used resulted in the production of GAG being significantly lower compared to experimental observations. Also, the GAG production rate parameter α used resulted in the tissue construct growing to almost three times its initial size. Experimental observations only show the construct to double its size in the same amount of time. These parameters need adjustment so as to get better agreement with experiments [7].

In future the effects of stress between the different phases would have to be considered, in particular the shear stress's involved as cell layers moving relative to each other. Also, the effect of mechanical loading on the construct will be investigated.

References

[1] Regenerative Medicine - A New Industry - A Grand Challenge, http://www.lboro.ac.uk/departments/mm/research/healthcare/remedigc/.

[2] Langer, R. and Vacanti, J.P., 1993, Tissue Engineering, Science, **260**, 920–926.

[3] Poiraudeau, S., Monteiro, I., Anract, P., Blanchard, O., Revel, M., and Corvol, T., 1999, Phenotypic characteristics of rabbit intervertebral disc cells: comparison with cartilage cells from the same animals, Spine, **24**, pp. 837–844.

[4] Chiba, K., Anderson, G. B. J., Masuda, K., and Thonar, E. J., 1997, Metabolism of the extracellular matrix formed by intervertebral disc cells cultured in alginate, Spine, **22**, pp. 2885-2893.

[5] Sato, M., Kikuchi, M., Ishihara, M., Ishihara, T., Asazuma, T., Kikuchi, T., Masuoka, M., Hattori, H., and Fujikawa, K., 2003, Tissue engineering of the intervertebral disc with cultured annulus fibrosus cells using atelocollagen honeycombshaped scaffold with a membrane seal (ACHMS scaffold), Med. Biol. Eng. Comput., **41**, pp. 365 – 371.

[6] Sengers, B.G., Taylor, M., Please, C.P., and Oreffo, R.O.C., 2007, Computational modelling of cell spreading and tissue regeneration in porous scaffolds, Biomaterials, **28**, 10, pp. 1926–1940.

[7] Obradovic, B., Meldon, J.H., Freed, L.E., and G. Vunjak-Novakovic, 2000, Glycosaminoglycan deposition in engineered cartilage: Experiments and mathematical model, Aiche J., **46**, 9, pp. 1860–1871.

[8] Truesdell, C., and Noll, W., 1960, The nonlinear field theory of mechanics, In: S. Flugge (ed.), Handbuch der Physik, Springer.

[9] Lemon, G., King, J.R., Byrne, H., Jensen, O.E., and Shakesheff, K.M., 2006, Mathematical modelling of engineered tissue growth using a multiphase porous flow mixture theory, J. Math. Biol., **52**, pp. 571–594.

[10] Lemon, G., and King, 2007, Multiphase modelling of cell behaviour on artificial scaffolds: effects of nutrient depletion and spatial non-uniform porosity, Math. Med. Biol., **24**,1, pp. 57–83.